

# Chapter 1

## Basics of EEG: Generation, Acquisition, and Applications of EEG



Chang-Hwan Im

**Abstract** The purpose of this chapter is to provide comprehensive knowledge about the generation and acquisition of electroencephalograms (EEGs), which is essential for understanding the following chapters. The physiological background on the generation of EEGs is presented, and then, a detailed description of the acquisition of EEG signals is given. Practical applications of computational EEG analysis are also introduced. Finally, the major advantages and limitations of current EEG technologies are discussed.

### 1.1 Generation of EEG

An electroencephalogram (EEG) is the flow of neuronal ionic currents recorded using a pair of electrodes either inside or outside the scalp. The EEG signal recorded inside the skull, referred to as the intracranial EEG (iEEG), can be used for surgical planning of intractable epilepsies [15]; however, this is not dealt with in this book (except in Chap. 8). Throughout this book, “EEG” refers to a *scalp EEG* recorded noninvasively from a pair of electrodes attached to the scalp surface.

In comparison with brain metabolism- or hemodynamics-based neuroimaging modalities, such as positron emission tomography (PET), functional magnetic resonance imaging (fMRI), and functional near-infrared spectroscopy (fNIRS), EEGs can offer excellent temporal resolution, allowing studies of neuronal dynamics occurring within a few milliseconds. However, the spatial resolution of an EEG is not comparable to that of an fMRI, owing to the small numbers of spatial data samplings, inherent volume conduction effect, and physiological and environmental noises/artifacts.

A first human EEG was recorded in 1924 by a German psychiatrist, Hans Berger. Despite the rapid technological developments, the basic methods for recording EEGs remain unchanged from Hans Berger’s era. An EEG measures electric potential differences between pairs of electrodes. The electrodes may be either directly attached

---

C.-H. Im (✉)

Department of Biomedical Engineering, Hanyang University, Seoul, South Korea  
e-mail: ich@hanyang.ac.kr

to the scalp surface at some specific locations or fitted in a cap (or a net) for more convenient attachment.

The main generators of the EEG, often referred to as *EEG sources*, are cortical neurons. It is well-documented that most neurons in the human brain are concentrated within the cerebral cortex, which is a thin sheet of gray matter with 2–4 mm thickness. The apical dendrites of the cortical neurons, often referred to as *large cortical pyramidal neurons*, are arranged almost perpendicularly to the surface of the cerebral cortex. Therefore, the direction of the neuronal current flowing along the long apical dendrites of cortical pyramidal neurons also becomes perpendicular to the cortical surface [10, 22]. This physiological basis can be used as an important constraint for EEG source imaging [1], which will be introduced in Chap. 5.

There are two different sorts of intracellular potentials that may potentially contribute to the generation of scalp EEG signals, which are an *action potential* and a *postsynaptic potential*. The action potential is elicited by sudden changes in transmembrane resting potential due to the dynamic movements of intracellular and extracellular ions, such as sodium, chloride and potassium ions. When the action potential within a neuron propagates to a synapse, a small gap junction between two neurons, the postsynaptic potential is generated across a pair of neighboring neuronal membranes. If the postsynaptic potential exceeds a threshold level, the action potential of one neuron is delivered to the other neuron (see Fig. 1.1).

Among the two different types of potentials, the postsynaptic potential is believed to contribute more to the generation of measurable extracranial electric fields than the action potential. This is because the action potentials do not fire synchronously in a large number of neurons [25]. On the contrary, although the magnitude of the postsynaptic potential is generally smaller than that of the action potential, its relatively longer duration (~30 ms) enables synchronous generation of the postsynaptic potentials in a large number of neurons (see Fig. 1.1). As aforementioned, since the apical dendrites of cortical pyramidal neurons are arranged almost perpendicularly to the cortical surface, the summation of the synchronously generated postsynaptic

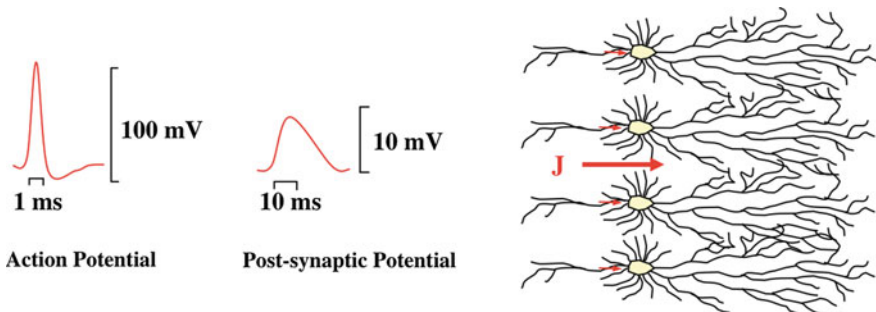


**Fig. 1.1** (Left) Comparison of waveforms of action potential and postsynaptic potential. (Right) Synchronous occurrence of postsynaptic potentials can produce unidirectional primary current flow large enough to be recorded outside the head

potentials in a small cortical area can induce extracranial electric fields large enough to be measured on the scalp surface [1]. According to Hämäläinen et al. [10], the current density on the cortical surface is approximately  $100 \text{ nA/mm}^2$ . When numerous cortical neurons within a small area are activated synchronously, a unidirectional neuronal current flow is formed. Figure 1.1 depicts the comparison between action potential and postsynaptic potential, as well as a schematic illustration of the generation of the unidirectional neuronal current flow.

The unidirectional neuronal currents, which can be approximately modeled as *equivalent current dipoles* (ECDs) in EEG source imaging problems [6] (see Chap. 5 for more details), are called *primary* or *impressed currents* [22]. Since the human body is filled with electrically conductive media, the extracellular currents induced by the primary currents can flow even to the farthest part of the human body. These extracellular currents are known as *secondary*, *volume*, or *return currents* [22]. According to the electromagnetic theories, the flow of the secondary currents results in nonuniform potential distributions on the scalp. The measurement of the potential difference between two distant scalp locations over time is the EEG.

Because the EEG measures dynamic changes in potential differences originating from the secondary current flows, precise evaluation of conductivity profiles of the volume conductors, i.e., different tissue compartments inside the head, is important, not only to understand the underlying mechanisms of the EEG, but also to build a precise head model to calculate electric field quantities generated by primary neuronal currents (this process is called *forward calculation*). A human head can be roughly modelled with four different regions: brain, cerebrospinal fluid (CSF), skull, and scalp. Table 1.1 shows the typical conductivity values when the conductivity of each region is assumed to be isotropic (having uniform conductivity in all directions) and homogeneous [9]. The most notable point in the conductivity profile shown in Table 1.1 is that the conductivity value of the skull is even smaller than those of the other tissues. Because of the poor electrical conductivity of the skull, the secondary currents are severely distorted and/or attenuated before they are delivered to the scalp surface. Since the tissue conductivity is an important factor affecting the reliability and accuracy of EEG source imaging, anisotropic conductivity characteristics are sometimes considered. For example, the skull has an anisotropic conductivity property, approximately  $0.014$  and  $0.0107 \text{ S/m}$  for the directions normal and tangential to the skull surface, respectively [2]. White matter tissues also have an anisotropic conductivity property: the white matter conducts secondary currents much better along a fiber direction than in its transverse directions [31]. In practice, however, a rough approximation of the human head structure as piecewise isotropic and homogeneous volume conductors (e.g., brain, CSF, skull, and scalp) is most widely used. More detailed discussion of this topic is provided in Chap. 5.

**Table 1.1** Typical conductivity values for different brain tissues/regions [9]

Regions	Absolute conductivity (S/m)	Relative conductivity
Brain	0.22	1
CSF	1.79	8
Skull	0.014	1/16
Scalp	0.22	1

## 1.2 Acquisition of EEG

Initial analog EEG devices recorded ongoing EEG activities on printed paper, when no quantitative EEG analysis was possible. Nowadays, owing to the development of computer technology and digital engineering, EEG signals are stored in computers as sampled numeric data. The use of a *digital EEG* enables us to utilize a variety of computational EEG analysis technologies, such as time-frequency analysis, functional connectivity analysis, and source imaging.

To record EEG data, at least two electrodes must be used, because EEG measures the potential difference between two distant scalp locations. Recent EEG recording devices allow simultaneous recording of EEG signals from many scalp locations. There are two types of EEG recording methods: *bipolar* and *unipolar* methods. In the bipolar method, electrodes are all paired, and the potential differences between each pair of electrodes are recorded. In the unipolar (or monopolar) method, the potential differences between each electrode and a reference electrode are recorded. Theoretically, the reference electrode in unipolar recording can be positioned anywhere; however, because the distribution of potential difference on the scalp surface varies according to the location of the reference electrode, *average reference* is frequently used. *Average-referenced* potential of each electrode can be readily evaluated by subtracting the average of all electrodes from the potential difference of each electrode. Average reference is particularly useful in depicting spatial distributions of potentials on the scalp surface, usually referred to as *topography* or *topographic map*.

EEG electrodes are generally attached on the scalp according to international standard configurations represented by the international 10–20 system. In the 10–20 system, electrodes are placed at 10 and 20% fractions of the geodesic distances between a number of anatomical landmarks such as inion, nasion, and two preauricular points. Smaller subdivisions (e.g., the 10–5 system) are also used for the placement of more electrodes. Further information on the electrode systems and electrode naming can be found in Oostenveld and Praamstra [24] and other sources—e.g., Wikipedia, [https://en.wikipedia.org/wiki/10–20\\_system\\_\(EEG\)](https://en.wikipedia.org/wiki/10–20_system_(EEG)).

In general, most EEG recording devices are composed of a signal amplifier, analog filter, and analog-to-digital converter (ADC). Use of high-quality signal amplifiers is necessary to display and process EEG signals on the order of microvolts. Since the recorded EEG signals are usually contaminated by unwanted environmental and/or systemic noises, such as alternating current (AC) power noises, a variety of electronic

circuits are implemented in the EEG amplifier to remove or reduce the noise. Analog filters can also be used to remove specific noise components and increase signal-to-noise ratio (SNR). High-pass and band-reject (*notch*) filters can be used optionally to reject low-frequency physiological noise (e.g., respiration artifact) and AC power noise, respectively. All EEG devices should include an analog low-pass filter with a cutoff frequency less than half of the sampling rate to prevent *aliasing*, unwanted distortion in the sampled EEG signal. This type of analog low-pass filter is generally referred to as the *anti-aliasing filter*. This will be dealt with in a more detailed manner in Chap. 3. ADC converts the amplified and filtered analog signals to digital EEG signals using sampling and encoding procedures [28].

### 1.3 Computational EEG Analysis

Once the digital EEG signals have been stored in storage media, a variety of forms of information characterizing the underlying brain activities can be extracted from the numeric data. In this book, four major computational EEG analysis methods are introduced: EEG spectral analysis (Chap. 3), event-related potential (ERP) analysis (Chap. 4), EEG source imaging (Chap. 5), and functional connectivity analysis (Chap. 6).

#### 1.3.1 EEG Spectral Analysis

One of the main advantages of EEG over the other hemodynamics- or neurochemistry-based neuroimaging modalities, such as fMRI and PET, is its superior temporal resolution that makes it possible to investigate neuronal activities changing on the order of tens of milliseconds. Thanks to the high temporal resolution of EEG, a large amount of useful information can also be obtained from frequency domain (or *spectral*) analysis. It is well known that changes in the EEG power spectrum are directly or indirectly associated with a variety of ongoing brain activities, e.g., mu-band (8–12 Hz) event-related desynchronization (ERD) and beta-band (18–22 Hz) event-related synchronization (ERS) associated with motor execution [11] and alpha-band (8–13 Hz) ERD associated with visual encoding [16]. EEG spectral analysis can also provide useful biomarkers to help diagnose and characterize various psychiatric diseases and neurological disorders. For example, reduced frontal gamma-band (30–50 Hz) activity may indicate declined cognitive function [3] and increased midline beta-band (13–30 Hz) activity may be an indicator of restless-leg syndrome [8, 14]. Spectral analysis can also be used to implement various types of brain–computer interfaces (BCIs) and neurofeedback systems [12].

### ***1.3.2 Event-Related Potential Analysis***

In the history of EEG, the most important advancement was the use of *stimulus-locked* averaging of event-related EEG. Using *event-related potentials* (ERP) analysis, one can observe spatiotemporal components of stimulus-locked brain electrical activities with reduced background noise. Examples of important ERP components include P300 [20], N170 [4], mismatch negativity (MMN) [17], and error-related negativity (ERN) [30], which have been widely used not only for cognitive/clinical neuroscience studies [21] but also for BCI applications [7]. A series of methods has recently been proposed to extract more precise spatiotemporal ERP waveforms with fewer repeated trials, and this will be introduced in a detailed manner in Chap. 4.

### ***1.3.3 EEG Source Imaging***

The limited spatial resolution of EEG can be substantially enhanced by performing *EEG source imaging*, or *electrical source imaging* (ESI), which estimates locations, directions, and/or distribution of EEG sources by solving mathematically defined problems called inverse problems [23]. To solve the inverse problems, a procedure for modeling the human head and calculating the relationship between EEG sources and scalp potentials is necessary. This procedure is generally referred to as *forward calculation* or *solving forward problems*. Because accurate forward calculation is important to obtain accurate inverse solutions, high-precision numerical methods, such as the boundary element method (BEM) and finite-element method (FEM), have been adopted. To solve the inverse problems, various algorithms and models have been proposed, each of which has its own advantages and drawbacks. Detailed descriptions of the methods for EEG forward/inverse problems can be found in Chap. 5.

### ***1.3.4 Functional Connectivity Analysis***

Traditional neuroscience studies focused on functional specification of brain areas; however, recent neuroimaging studies exhibited increased interest in the functional connectivity among different brain areas. EEG is especially useful to study functional connectivity between two recording sites (or brain areas after EEG source imaging) because of its high temporal resolution. There are different kinds of functional connectivity measures that have been actively applied to EEG analyses, such as coherence, phase-locking value (PLV), phase lag index (PLI), Granger's causality (GC), and partial directed coherence (PDC). Functional connectivity analysis has proved to be useful to characterize various psychiatric diseases. Indeed, several recent studies have shown disrupted or abnormal functional connectivity patterns in patients with psychiatric illnesses; examples include schizophrenia [27], mild cogni-

tive impairment [26], and post-traumatic stress disorder [13]. In particular, functional connectivity analysis is useful to study epilepsy because epilepsy is thought to be one of the most representative *brain network disorders* [18]. Detailed descriptions of the functional connectivity measures can be found in Chap. 6.

## 1.4 Applications of EEG

In the early stage of development of EEG, visual inspection of EEG waveforms was the only way to use EEG in practical applications. Indeed, visual inspection of EEG waveforms is still useful in studying sleep and diagnosing some neurological disorders, such as epilepsy. Dissemination of digital EEGs expanded the application fields of EEGs from limited research and diagnostic applications to more-extensive applications, including cognitive neuroscience study, diagnosis of psychiatric diseases, neuromarketing, neuroergonomics, sports science, and human brain mapping. Recently, owing to the rapid development of digital engineering, EEGs can be applied to real-time applications, such as BCI and neurofeedback.

The use of EEG in practical applications has steadily increased and is expected to continue to increase. Indeed, EEG has many advantages over the other methods to study brain functions, as follows:

- EEG is perfectly noninvasive, without any exposure to radiation or high magnetic field
- EEG is economical
- EEG devices can be made small and portable
- EEG has high temporal resolution
- EEG devices do not generate any noise
- EEG can be recorded in an open environment
- EEG can be acquired without active response from subjects.

Traditionally, EEG data were acquired in laboratory or clinical environments, where there are high-end EEG recording devices with a large number of channels and well-motivated participants who have agreed to participate in experiments with long durations. Recently, however, the advancement of wireless technology and high-performance biosensors enabled the development of wearable EEG devices that are easy to wear and comfortable for long-term use, expediting the development of novel applications of EEG that do not necessarily require laboratory settings, e.g., monitoring the brain activity of healthy persons during daily life [5, 19, 29].

Despite the recent development of EEG technology, EEG still has some intrinsic limitations that need to be overcome, examples of which include low spatial resolution and low SNR. Therefore, development of new computational EEG analysis methods is still necessary to enhance the reliability and usability of EEG.

## References

1. S. Baillet, J.C. Mosher, R.M. Leahy, Electromagnetic brain mapping. *IEEE Signal Process. Mag.* **18**, 14–30 (2001)
2. S. Baillet, J.J. Riera, G. Marin, J.F. Mangin, J. Aubert, L. Garnero, Evaluation of inverse methods and head models for EEG source localization using a human skull phantom. *Phys. Med. Biol.* **46**, 77–96 (2001)
3. E. Başar, A review of gamma oscillations in healthy subjects and in cognitive impairment. *Int. J. Psychophysiol.* **90**, 99–117 (2013)
4. V.C. Blau, U. Maurer, N. Tottenham, B.D. McCandliss, The face-specific N170 component is modulated by emotional facial expression. *Behav. Brain Funct.* **3**, 7 (2007)
5. W.D. Chang, H.S. Cha, K. Kim, C.H. Im, Detection of eye blink artifacts from single prefrontal channel electroencephalogram. *Comput. Methods Programs Biomed.* **124**, 19–30 (2016)
6. J.C. de Munck, B.W. van Dijk, H. Spekreijse, Mathematical dipoles are adequate to describe realistic generators of human brain activity. *IEEE Trans. Biomed. Eng.* **35**(11), 960–966 (1988)
7. R. Fazel-Rezai, B.Z. Allison, C. Guger, E.W. Sellers, S.C. Kleih, A. Kübler, P300 brain computer interface: current challenges and emerging trends. *Front Neuroeng.* **5**, 14 (2012)
8. D.C. Hammond, Neurofeedback treatment of restless legs syndrome and periodic leg movements in sleep. *J. Neurother.* **16**(2), 155–163 (2012)
9. J. Haueisen, C. Ramon, M. Eiselt, H. Brauer, H. Nowak, Influence of tissue resistivities on neuromagnetic fields and electric potentials studied with a finite element model of the head. *IEEE Trans. Biomed. Eng.* **44**(8), 727–735 (1997)
10. M.S. Hämäläinen, R. Hari, R.J. Ilmoniemi, J. Knuutila, O.V. Lounasmaa, Magnetoencephalography. Theory, instrumentation and applications to the noninvasive study of human brain function. *Rev. Mod. Phys.* **65**, 413–497 (1993)
11. H.J. Hwang, K. Kwon, C.H. Im, Neurofeedback-based motor imagery training for brain-computer interface (BCI). *J. Neurosci. Meth.* **179**(1), 150–156 (2009)
12. H.J. Hwang, S. Kim, S. Choi, C.H. Im, EEG-based brain-computer interfaces: a thorough literature survey. *Int. J. Hum. Comput. Interact.* **29**(12), 814–826 (2013)
13. C. Imperatori, B. Farina, M.I. Quintiliani, A. Onofri, P. Castelli Gattinara, M. Lepore, V. Gnoni, E. Mazzucchi, A. Contardi, G. Della Marca, Aberrant EEG functional connectivity and EEG power spectra in resting state post-traumatic stress disorder: a sLORETA study. *Biol. Psychol.* **102**, 10–17 (2014)
14. K.Y. Jung, Y.S. Koo, B.J. Kim, D. Ko, G.T. Lee, K.H. Kim, C.H. Im, Electrophysiologic disturbances during daytime in patients with restless legs syndrome: further evidence of cognitive dysfunction? *Sleep Med.* **12**(4), 416–421 (2011)
15. Y.J. Jung, H.C. Kang, K.O. Choi, J.S. Lee, D.S. Kim, J.H. Cho, S.H. Kim, C.H. Im, H.D. Kim, Localization of ictal onset zones in Lennox-Gastaut syndrome using directional connectivity analysis of intracranial electroencephalography. *Seizure* **20**(6), 449–457 (2011)
16. W. Klimesch, R. Fellinger, R. Freunberger, Alpha oscillations and early stages of visual encoding. *Front. Psychol.* **2**, 118 (2011)
17. D. Ko, S. Kwon, G.T. Lee, C.H. Im, K.H. Kim, K.Y. Jung, Theta oscillation related to the auditory discrimination process in mismatch negativity: oddball versus control paradigm. *J. Clin. Neurol.* **8**(1), 35–42 (2012)
18. C. Lee, S.M. Kim, Y.J. Jung, C.H. Im, D.W. Kim, K.Y. Jung, Causal influence of epileptic network during spike-and-wave discharge in juvenile myoclonic epilepsy. *Epilepsy Res.* **108**(2), 257–266 (2014)
19. C.T. Lin, L.D. Liao, Y.H. Liu, I.J. Wang, B.S. Lin, J.Y. Chang, Novel dry polymer foam electrodes for long-term EEG measurement. *IEEE Trans. Biomed. Eng.* **58**, 1200–1207 (2011)
20. D.E. Linden, The p300: where in the brain is it produced and what does it tell us? *Neuroscientist* **11**(6), 563–576 (2005)
21. S.J. Luck, *An Introduction to the Event-Related Potential Technique* (The MIT Press, Boston, 2005)



22. J. Malmivuo, R. Plonsey, *Bioelectromagnetism* (Oxford University Press, Oxford, 1995)
23. P.L. Nunez, R. Srinivasan, *Electric Fields of the Brain: The Neurophysics of EEG* (Oxford University Press, Oxford, 2006)
24. R. Oostenveld, P. Praamstra, The five percent electrode system for high-resolution EEG and ERP measurements. *Clin. Neurophysiol.* **112**, 713–719 (2001)
25. W.W. Orrison, J.D. Lewine, J.A. Sanders, M.F. Hartshorne, *Functional Brain Imaging* (Mosby, Maryland Heights, 1995)
26. Y.A. Pijnenburg, Y. Vd Made Y, A.M. van Walsum, D.L. Knol, P. Scheltens, C.J. Stam, EEG synchronization likelihood in mild cognitive impairment and Alzheimer’s disease during a working memory task. *Clin. Neurophysiol.* **15**(6), 1332–1339 (2004)
27. M. Shim, D.W. Kim, S.H. Lee, C.H. Im, Disruptions in small-world cortical functional connectivity network during an auditory oddball paradigm task in patients with schizophrenia. *Schizophr. Res.* **156**(2), 197–203 (2014)
28. M. Teplan, Fundamentals of EEG measurement. *Meas. Sci. Rev.* **2**(2), 1–11 (2002)
29. Y. Yasui, A brainwave signal measurement and data processing technique for daily life applications. *J. Physiol. Anthropol.* **28**, 145–150 (2009)
30. J.R. Wessel, Error awareness and the error-related negativity: evaluating the first decade of evidence. *Front. Hum. Neurosci.* **6**, 88 (2012)
31. C.H. Wolters, A. Anwander, X. Tricoche, D. Weinstein, M.A. Koch, R.S. MacLeod, Influence of tissue conductivity anisotropy on EEG/MEG field and return current computation in a realistic head model: a simulation and visualization study using high-resolution finite element modeling. *Neuroimage* **30**(3), 813–826 (2006)